

Anti-corrosion potential of the low-pressure nitriding method for the iron alloys

Emilia Wołowiec-Korecka^{1*} , Jerzy Michalski², Piotr Lipiński³

¹ Institute of Materials Science and Engineering, Lodz University of Technology, 1/15 B. Stefanowskiego Str. 1/15, Lodz 90537, Poland

² Faculty of Production Engineering, Warsaw University of Life Sciences, 164 Nowoursynowska Str., Warsaw 02787, Poland

³ Institute of Information Technology, Lodz University of Technology, 8 Politechniki Av., Lodz, 93590, Poland

* Corresponding author's e-mail: emilia.wolowiec-korecka@p.lodz.pl

ABSTRACT

This study aims to analyse the low-pressure nitriding method to determine its anti-corrosion protection potential. Components made of EN C20, EN 41CrAlMo7 and EN 42CrMo4 steels were low-pressure nitrided in a pure ammonia atmosphere at a pressure of 26 hPa. The nitrided layers formed were analysed in terms of structure, effective layer thickness, corrosion resistance and friction wear resistance. It was determined that an iron nitride layer with a phase composition of $\epsilon+\gamma'$ and a thickness of not less than 10 μm provides effective protection against the corrosive influence of the urban environment for up to 3 months, while layers with a thickness of not less than 14 μm provide effective protection for up to 5 months. The iron nitride layer was found to increase the friction wear resistance of the nitrided steel. The wear that occurs within the iron nitride layer is linear. The wear process, after exceeding the thickness of the iron nitride layer, progresses to an accelerated wear phase, which ultimately leads to seizure.

Keywords: thermochemical treatment, nitriding, corrosion resistance, vacuum, tool steels

INTRODUCTION

Nitriding is used to increase the hardness and friction wear resistance of the surface of machine parts and tools (1). Nitrided layers increase the corrosion resistance of products operating in less aggressive environments (unheated buildings, urban and industrial environments with moderate pollution, and, after impregnation, also of products operating in highly aggressive corrosive environments (salt mines, copper mines, industrial areas with high humidity and aggressive atmospheres) (2). The higher and higher requirements that arise from operating conditions require the manufacture of nitrided layers to be engineered with assumed structural characteristics. This implies designing a process that enables the production of such a layer. To effectively control the result of the nitriding process, it is necessary to control the nitrogen flux to the nitrided surface. Controlling and adjusting

the composition of the inlet atmosphere is a significant factor in controlling the nitrogen flux from the nitriding atmosphere to the nitrided surface and, consequently, the kinetics of the growth of the nitrided layer thickness (3).

According to the AMS 2759/10A standard, the nitrided layers can be classified into the following three types of layers (4):

- a solution of nitrogen in α -iron ($Fe_{\alpha(N)}$) without a superficial layer of iron nitrides,
- a mixture of Fe_4N (γ') and $Fe_{2-3}N$ (ϵ) ($\epsilon+\gamma'$) iron nitrides up to 15 μm thick with a superficial layer of iron nitrides,
- a mixture of Fe_4N (γ') and $Fe_{2-3}N$ (ϵ) iron nitrides with a 17–25 μm thick superficial layer of iron nitrides of the $\epsilon+(\epsilon+\gamma')$ structure.

Nitrided layers with a superficial layer of $\epsilon+(\epsilon+\gamma')$ iron nitrides after impregnation of the porous ϵ zone guarantee corrosion resistance in highly

aggressive corrosive environments (salt mines, copper mines, industrial areas with high humidity and an aggressive atmosphere). Nitrided layers with a superficial layer of $\epsilon+\gamma'$, and $\epsilon+(\epsilon+\gamma')$ iron nitrides without impregnation guarantee corrosion resistance in less aggressive environments (unheated buildings, urban and industrial environments with moderate pollution). The corrosion process of nitrided products has a pit-forming dynamics, the iron nitride layer gets passivated and the steel substrate corrodes. The intensity of the corrosion degradation process, depends on the thickness and the structure of the iron nitride layer.

Nitriding methods and their potential for corrosion protection of iron alloys have been widely discussed in the literature (5,6). The low-pressure nitriding method described in the work of Kula, Wolowiec-Korecka et al. (7) has been developed for hardening the top layer of tool steels. It so far has not been investigated for its anti-corrosion potential. The present study aims to analyse the atmospheric corrosion and friction wear resistance of nitrided layers with a superficial layer of $\epsilon+\gamma'$ iron nitrides and a layer thickness of less than 10 μm produced on EN C20, EN 41CrAlMo7 and EN 42CrMo4 steel components by low-pressure nitriding.

MATERIAL AND METHOD

The tested material included cylinders with diameters of 12 mm, 14 mm, 18 mm and the length of 80 mm made from EN 42CrMo4, EN 41CrAlMo7 and EN C20 steels and cylinders with

diameters of 8 mm and the length of 35 mm made from EN 42CrMo4 and EN 41CrAlMo7 steels. Table 1 shows the chemical composition of the steels used in the tests. The alloy steel pieces were heat treated before the nitriding process and the non-alloy steel pieces were normalised (Table 2).

Low-pressure nitriding processes were carried out in a multi-purpose vacuum furnace (Seco/Warwick, Poland) with a process space of 400×400×600 mm. The nitriding atmosphere used was ammonia (NH_3) of 99.99999% purity (The studies used analytical-grade ammonia because technical ammonia did not provide the desired results.). Nitriding was carried out at 560 °C for 2, 4 and 6 h, at a pressure of 26 hPa and an ammonia flow rate of 15 dm^3/min . After the nitriding process, the samples were cooled with nitrogen at 0.2 MPa to 50 °C. Metallographic images were taken of each element in planes perpendicular and parallel to the sample axis, following the procedure described in Betiuk et al.. Surface hardness was measured on the side surface of the cylinder, while the hardness distribution was measured on a cut perpendicular to the cylinder axis. The cut made in a plane perpendicular to the sample axis revealed the actual thickness of the iron nitride layer. If the cut was made in a plane parallel to the sample axis, in this case by grinding a cylinder section thicker than the surface layer of iron nitrides, a layer of iron nitrides thicker than the actual thickness was revealed as a result of geometric magnification (9). Photographs of the structures were taken at ×50, ×200 and ×500 magnifications.

Table 1. Chemical composition of steels used in tests

EN C20								
Element	C	Mn	Si	P	S	Cr	Ni	Cu
Wt. %	0.19	0.4	0.25	0.03	0.03	0.25	0.2	0.15
EN 42CrMo4								
Element	C	Mn	Si	P	S	Cr	Ni	Mo
Wt. %	0.4	0.6	0.2	0.02	0.03	1.1	0.3	0.25
EN 41CrAlMo7								
Element	C	Mn	Si	P; S	Cr	Ni	Mo	Al
Wt. %	0.38	0.5	0.3	0.025	1.5	0.25	0.2	1.0

Table 2. Parameters of steel heat treatment before nitriding process

Treatment params	41CrAlMo7	42CrMo4	C20 (20) steel
Quenching	Austenization: 20 min, 920 °C, oil-cooled	Austenization: 20 min, 840 °C, oil-cooled	Austenization: 40 min, 900 °C, air-cooled
Tempering	600 °C, 2 h, air-cooled	600 °C, 2 h, air-cooled	–

The structures of the nitrided layers were examined under an optical microscope (Neophot 2; Zeiss) to measure the thickness of the superficial iron nitride layer (CD_{wl} , white layer) and the effective diffusion zone thickness ($CD_{core+50HV}$). The distance from the surface where the hardness is equal or higher than the hardness of the core plus 50 $HV_{0.5}$ was adopted a criterion for the thickness of the effective diffusion zone of the nitrided steels. Nitrogen distribution profile in the nitrided layer was tested using a spectrometer (GDOS 850A, LECO) (GDOES - Glow Discharge Optical Emission Spectroscopy). The corrosion resistance of the nitrided steels was tested under atmospheric corrosion conditions at the urban environment corrosion test station according to the PN-EN ISO 9223:2012 standard (10). The test samples were placed on an exposure frame; the clamping method prevented contact between adjacent samples and ensured electrical insulation between the samples and the frame. The degree of corrosion was assessed visually after one, three, four and five months according to the recommendations of the standard PN ISO 4628-1:2005 (11).

Friction wear resistance was tested in accordance with the PN-83/H-04302 standard (12). Friction wear was described by total linear wear as a function of friction path. Figure 1 shows a diagram of a friction pair in a 3-roller-cone system. This system is a modification of the four-ball test method, with the difference that here, one rotating ball was replaced by a rotating cone and three

stationary balls by three stationary rollers. The tests were performed with continuous lubrication of the samples, at a constant rotational speed n of the cone equal to 9.6 s^{-1} and a specified unit pressure. The wear depth was determined based on measurements of the diameters (a_1 and b_1) of the ellipse created by wear on the surface of each roller and averaging the measurement results. The total test time was 100 min. The wear was measured by interrupting the test every 10 min, and then the load was increased in proportion to the increasing wear area. The wear due to friction was characterized by the total linear wear during the steady-state wear period. The wear depth Z_l , defining the linear wear, was calculated from the equation:

$$Z_l = 0.5 \cdot \left[D - \sqrt{D^2 - \left(\frac{\sum(a_1 + b_1)}{6} \right)^2} \right] \quad (1)$$

where: D – diameter of the cone in the friction node, a_1, b_1 – large and small diameter of the ellipse, respectively.

RESULTS

Structure of nitrided layers

The iron nitride layers obtained on EN C20, EN 42CrMo4, EN 41CrAlMo7 steels were of uniform thickness; their thickness grew as the nitriding process time increased (Fig. 2, 3, 4). The thickness of the iron nitride layers found in the

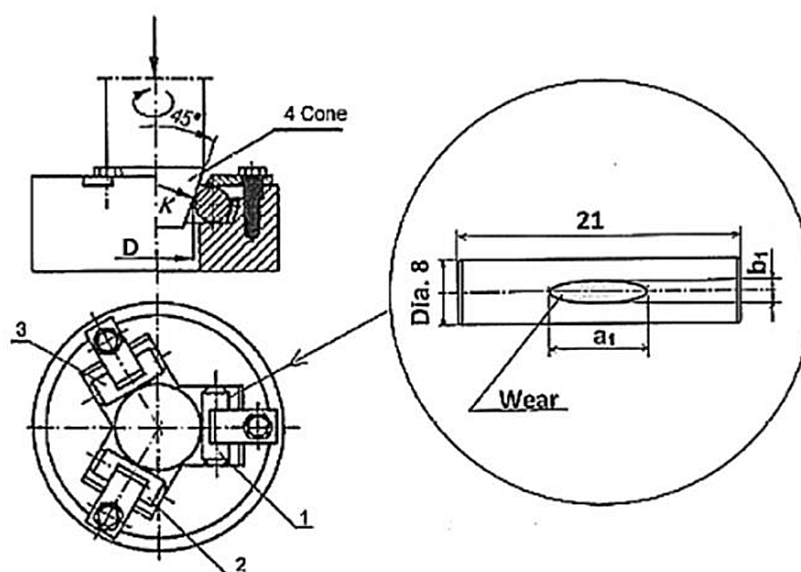


Figure 1. Schematic diagram of the friction pair in the 3-roller-cone system: 1,2, 3 – stationary rollers during the test, 4 – rotating cone, D – diameter of the cone in the friction node (12)

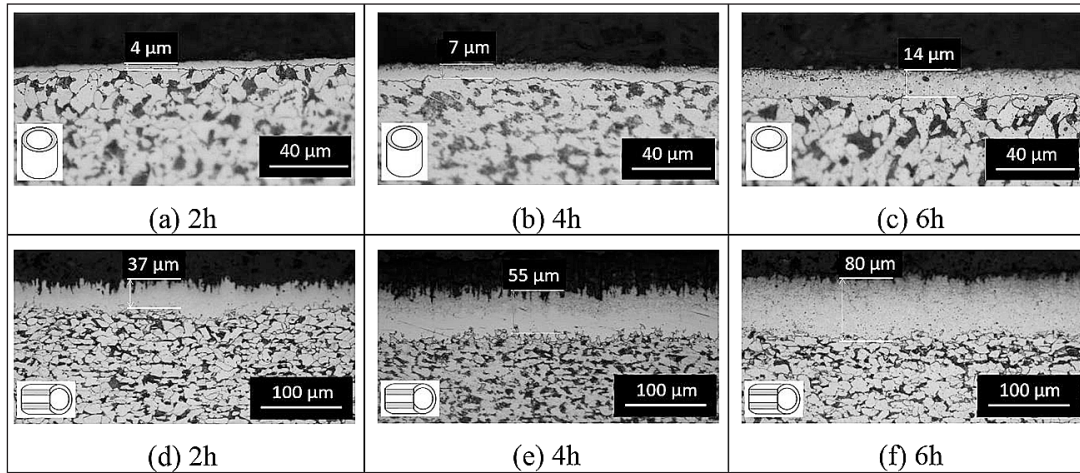


Figure 2. The microstructures of EN C20 steel samples after low-pressure nitriding; temperature 560 °C, pressure 26 hPa, duration 2 h (a, d), 4 h (b, e), 6 h (c, f). Microstructure in the plane perpendicular to the sample axis (a, b, c), microstructure in the plane parallel to the sample axis (d, e, f)

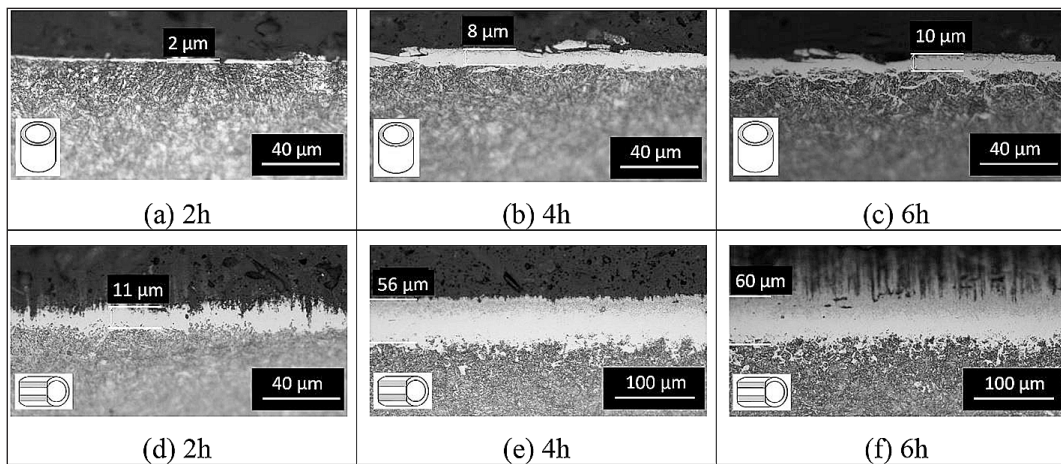


Figure 3. The microstructures of EN 42CrMo4 steel samples after low-pressure nitriding; temperature 560 °C, pressure 26 hPa, duration 2 h (a, d), 4 h (b, e), 6 h (c, f). Microstructure in the plane perpendicular to the sample axis (a, b, c), microstructure in the plane parallel to the sample axis (d, e, f)

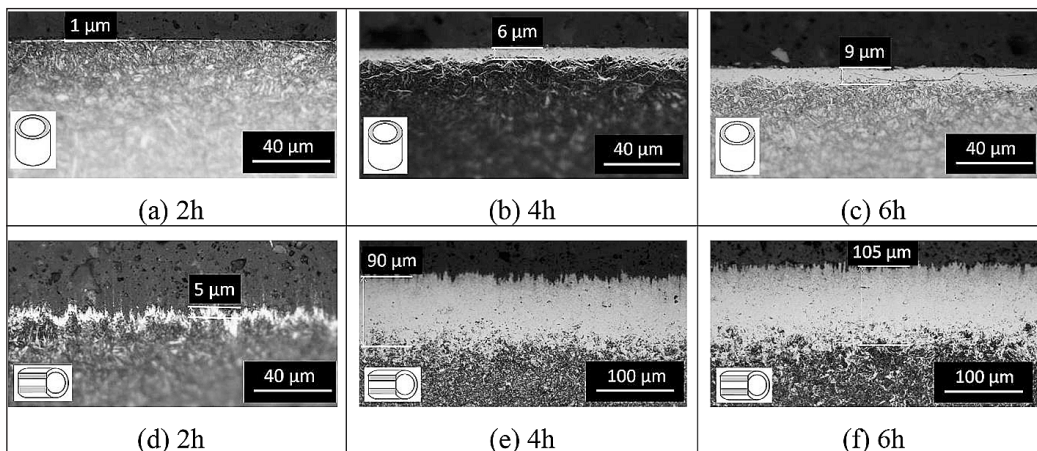


Figure 4. The microstructures of EN 41CrAlMo7 steel samples after low-pressure nitriding; temperature 560 °C, pressure 26 hPa, duration 2 h (a, d), 4 h (b, e), 6 h (c, f). Microstructure in the plane perpendicular to the sample axis (a, b, c), microstructure in the plane parallel to the sample axis (d, e, f)

plane parallel to the sample axis (Fig. 2, 3, 4 d, e, f) was several times greater than the thickness of the layer found in the plane perpendicular to the sample axis (Fig 2, 3, 4 a,b,c). The thickest iron nitride layers after 6 h of the nitriding process were observed for EN C20 steel, the thinnest on EN 41CrAlMo7 steel (Fig. 5a). The surface hardnesses of EN 42CrMo4 and EN 41CrAlMo7 steels (Fig. 5b) were lower than those obtained in the process of gas nitriding at normal pressure (1013 hPa) over comparable periods of time. This was also true for the effective case depth ($CD_{core+50HV}$) (Fig. 5c).

Nitriding elements (Cr, Mo, Al) present in heat-treatable steels significantly affect the thickness and properties of nitrided layers. Carbides of nitriding elements present in EN 42CrMo4 and EN 41CrAlMo7 steels, in reaction with diffusing nitrogen, form carbonitrides and cause an increase in the hardness of the nitrided steel surface. The surface hardness increases with the increase in the content of nitriding elements, which is why higher hardness is obtained on EN 41CrAlMo7 steel than on EN 42CrMo4 steel (Fig. 5b). On the other hand, the increase in the content of nitriding elements limits the range of nitrogen diffusion

into the substrate and limits the effective thickness of the diffusion layer (Fig. 5c). For this reason, the obtained effective thickness $g_{core+50}$ of the solution zone is smaller in EN 41CrAlMo7 steel than in EN 42CrMo4 steel. The alloying elements in the above-mentioned steels increase the absorptivity of the steel and therefore thinner iron nitride layers were formed on EN 41CrAlMo7 and EN 42CrMo4 than on EN C20 steel, which has no other alloying elements apart from carbon (Fig. 6). Using the Fe-N equilibrium system (13), the structure of the nitrided layer was proposed (Fig. 7). In the case of unalloyed steel EN C20 (Fig. 7a), up to approx. 2 μm from the surface, the nitrogen concentration decreases from 12 to 8 wt.% N, which proves that the dominant phase in this zone is the ϵ phase, then the concentration decreases to 6 wt.% N and maintains almost constant up to the boundary with the substrate, i.e. up to 14 μm from the surface, where the dominant phase in this zone is the γ' phase. In the diffusion zone, the nitrogen concentration decreases very quickly and reaches a value of 0.3 wt.%, at a distance of 16 μm from the surface and does not change any more. Nitrogen in the diffusion zone can occur in ferrite and precipitation of the γ'

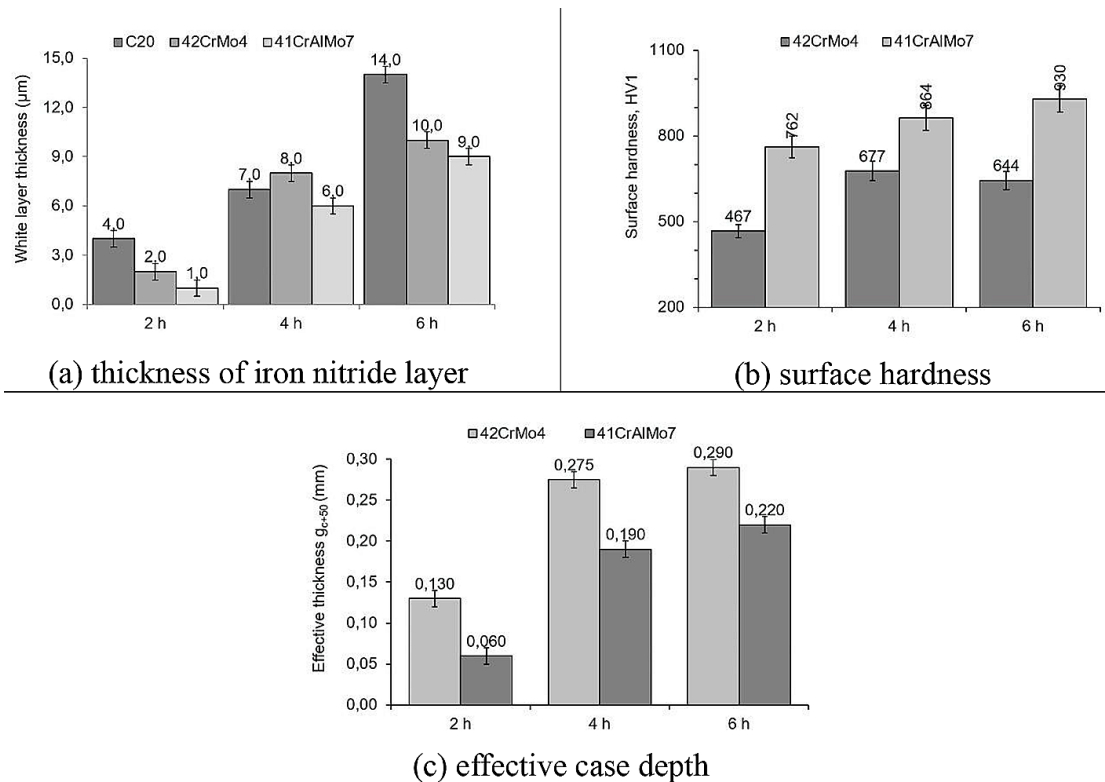


Figure 5. Properties of nitrided layers produced on EN C20, EN 42CrMo4, EN 41CrAlMo7 steels after low-pressure nitriding at 2 h, 4 h and 6 h. a) thickness of iron nitride layer, b) surface hardness of EN 42CrMo4 and EN 41CrAlMo7 steels, c) effective case depth (thickness, $CD_{core+50HV}$)

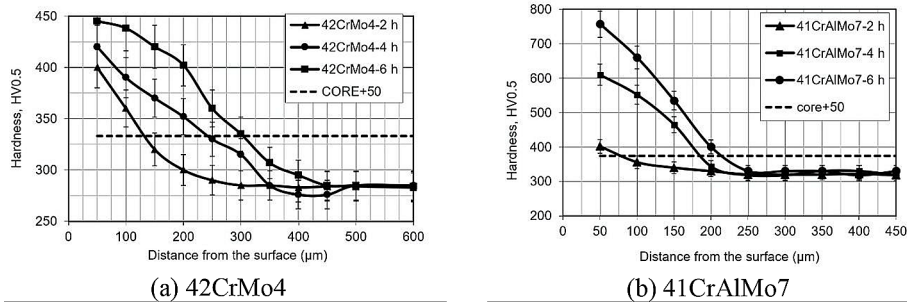


Figure 6. Hardness distribution in the nitrided layer after low-pressure nitriding for 2 h, 4 h, 6 h: a) EN 42CrMo4 steel, b) EN 41CrAlMo7 steel

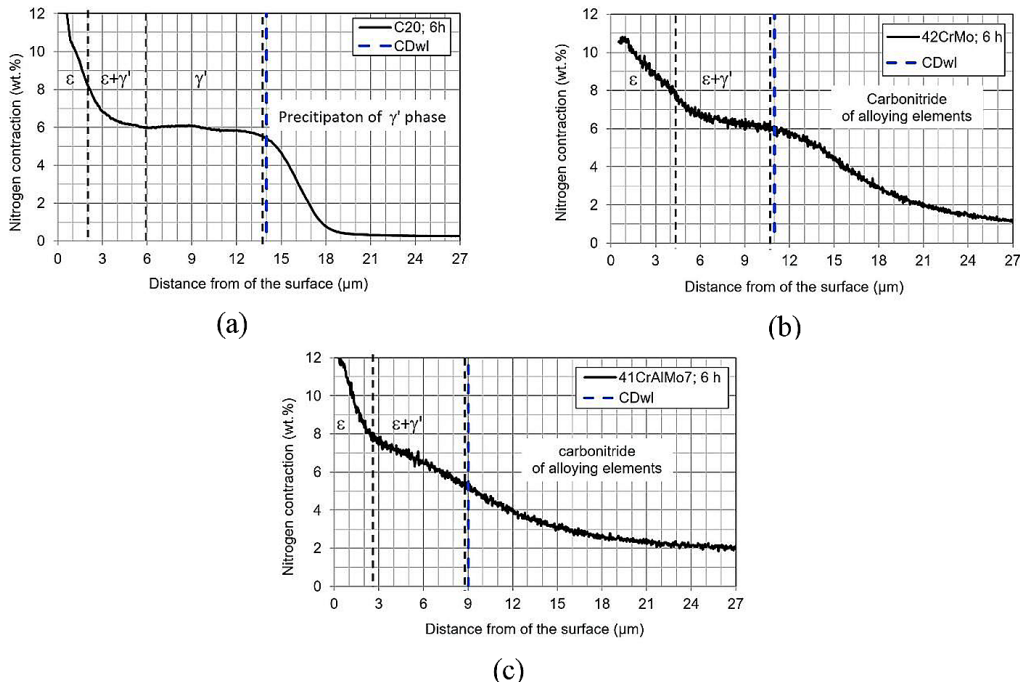


Figure 7. Distribution of nitrogen concentration in the nitrided layers after 6 hours of low-pressure nitriding under pressure 26 hPa: a) EN C20, b) EN 42CrMo4, c) EN 41CrAlMo7, CDwl – case depth (thickness) of the iron nitride layer

phase. The presence of nitride-forming elements (Cr, Mo, Al) makes it impossible to clearly indicate the boundary between the nitride layer and the substrate (Fig. 7b, c). In EN 42CrMo4 steel, up to about 4 μm from the surface, the nitrogen concentration decreases from about 11 to 8 wt.% N, which proves that the ε phase is the dominant phase in this zone. In the zone from 4 to 11 μm, the nitrogen concentration decreases to 6 wt.% N, which indicates that a mixture of ε and γ' phases occurs in this zone. Nitrogen occurs primarily in the carbonitrides of alloying elements in the diffusion zone. In EN 41CrAlMo7 steel, up to about 3.5 μm from the surface, the nitrogen concentration decreases from about 12 to 8 wt.%

N, which proves that the ε phase is the dominant phase in this zone. In the zone 3.5 to 9 μm, the nitrogen concentration decreases to 5.5 wt.% N, which indicates that a mixture of ε and γ' phases occurs in this zone. In the diffusion zone, nitrogen occurs primarily in the carbonitrides of alloying elements.

Corrosion protection properties

Figure 8, 9, 10 present the surfaces of the nitrided samples after exposure at the corrosion test station. In the case of EN C20 and EN 42CrMo4 steels, which were nitrided for 2 h, clear corrosion traces were observed after 4 months of exposure;

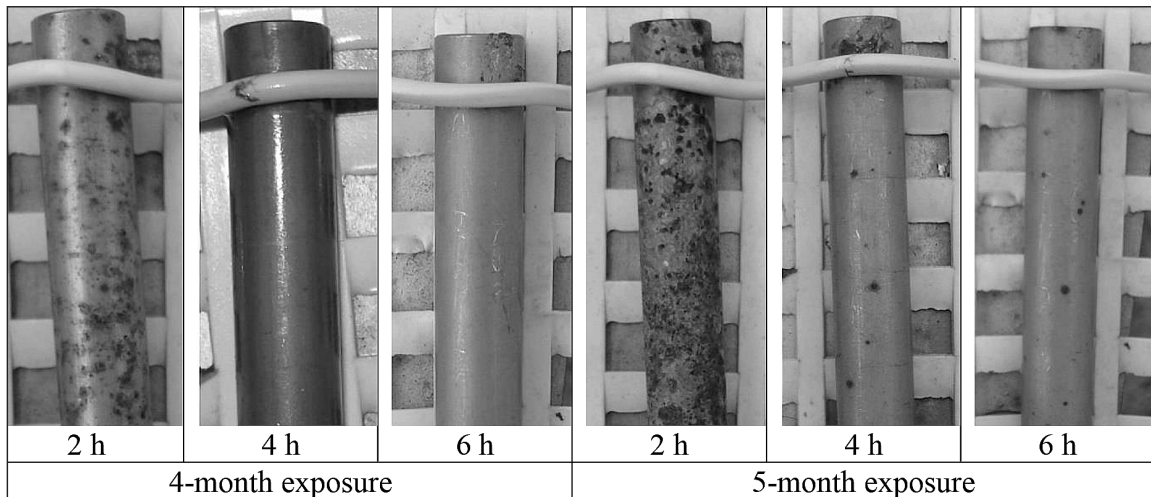


Figure 8. Surface of nitrided EN C20 steel components after exposure at the corrosion test station. Process: low-pressure nitriding 560 °C, pressure 26 hPa, duration 2 h, 4h and 6 h

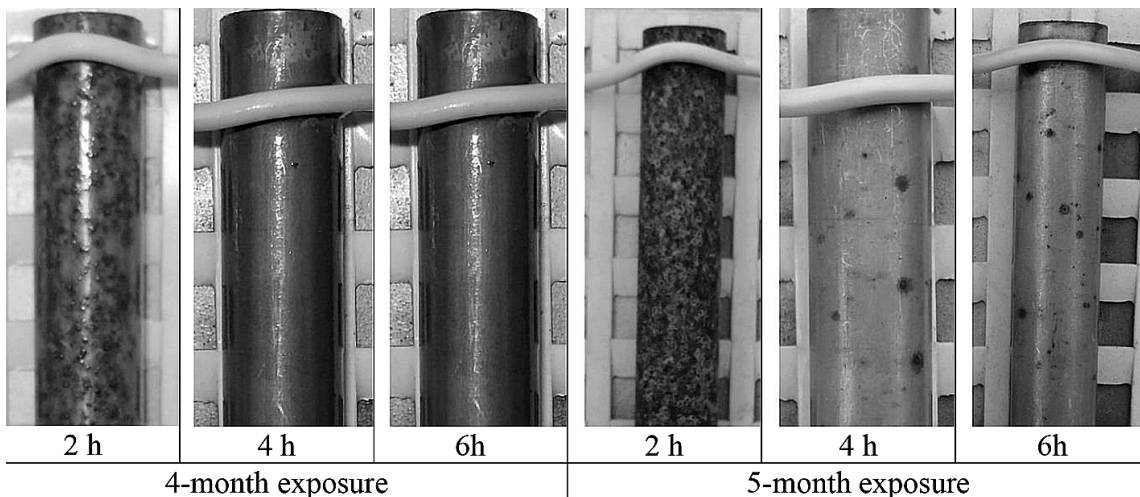


Figure 9. Surface of nitrided EN 42CrMo4 steel components after exposure at the corrosion test station. Process: low-pressure nitriding 560 °C, pressure 26 hPa, duration 2 h, 4 h and 6 h

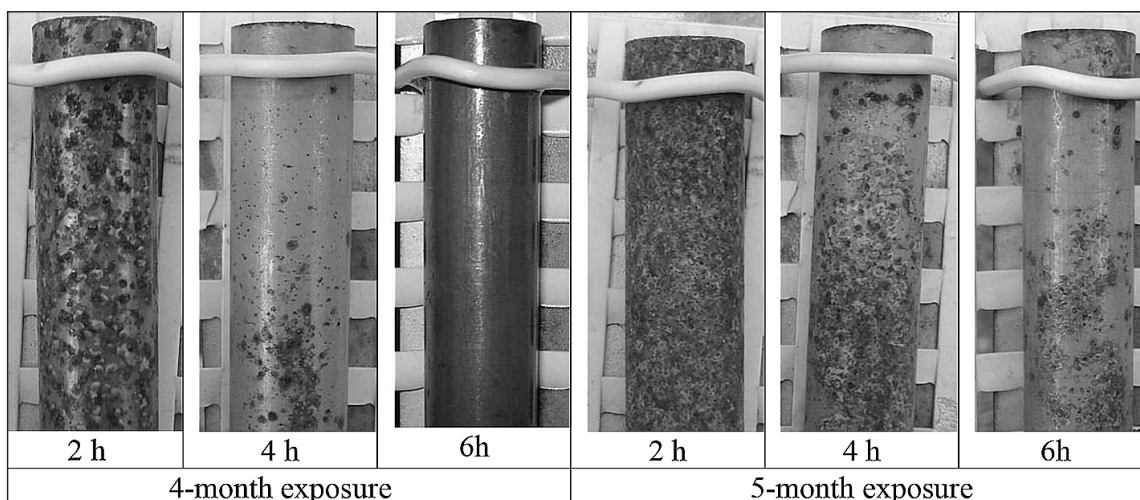


Figure 10. Surface of nitrided EN 41CrAlMo7 steel components after exposure at the corrosion test station. Process: low-pressure nitriding 560 °C, pressure 26 hPa, duration 2 h, 4 h and 6 h

whereas, for elements nitrided for 4 h and 6 h, single corrosion pits were found only after 5 months of exposure (Fig. 8, Fig. 9). For EN 41CrAlMo7 steel nitrided for 2 h, corrosion was found after one month of exposure, for the one nitrided for 4 h – after 3 months, and for the one nitrided for 6 h – after 5 months of exposure (Fig. 10). Table 3 shows the visual assessment results of the degree of destruction of the nitride layer after exposure to the corrosion station.

Friction wear

Figure 11 presents graphs of linear wear as a function of friction path for nitrided components made of EN 42CrMo4 (Fig. 11a) and EN 41CrAlMo7 (Fig. 11b) steels. The iron nitride layer noticeably increased the friction wear resistance. The iron nitride layer was worn off for the friction path of 4750 m at unit pressures of 200 MPa. The

wear at unit pressures of 100 MPa and 200 MPa was constant (linear) throughout the entire test. At 400 MPa unit pressures, accelerated wear was observed from the beginning of the test.

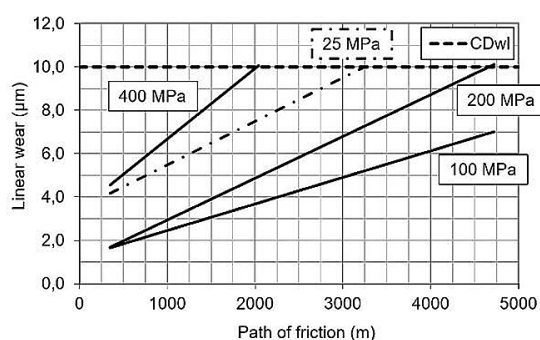
DISCUSSION

The iron nitride layers obtained on the EN C20 steel were of uniform thickness. No separation of the γ' phase in the ferrite grains was observed in the substrate, which usually occurs in layers nitrided using gas nitriding under atmospheric conditions. The results obtained for EN 42CrMo4 steel were similar to those obtained in the studies of Jordan (14), which present tests results of nitriding of the same steel. The surface hardnesses obtained on EN 42CrMo4 and EN 41CrAlMo7 steels were slightly lower than those obtained on the same steels in conventional processes at atmospheric

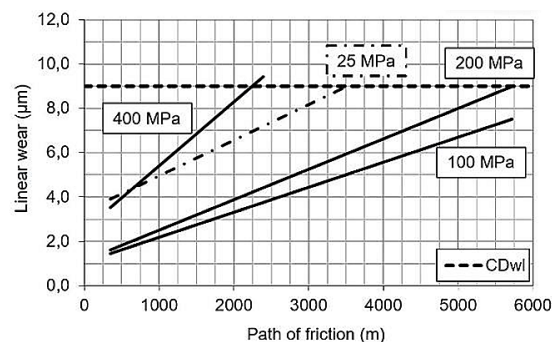
Table 3. Assessment of the degree of destruction of the nitride layer according to the PN ISO 4628-1:2005 standard (11)

Steel	Nitriding time	1 month	3 months	4 months	5 months
C20	2 h	1	2	3	4
	4 h	0	0	0	2
	6 h	0	0	0	2
42CrMo4	2 h	2	3	4	5
	4 h	0	0	3	4
	6 h	0	0	0	3
41CrAlMo	2 h	3	4	4	5
	4 h	1	3	2	4
	6 h	0	0	0	3

Note: 0 – none, i.e. no noticeable damage; 1 – very few, i.e. small, barely noticeable number of damages; 2 – few, i.e. small but noticeable number of damages; 3 – moderate number of damages; 4 – a significant number of damages; 5 – a dense pattern of damages.



(a) 42CrMo4



(b) 41CrAlMo7

Figure 11. Linear wear as a function of friction path for different friction test pressures. (a) EN 42CrMo4 steel, (b) EN 41CrAlMo7 steel. Solid lines – nitrided steels, dashed line – non-nitrided steels, CD_{wl} – case depth (thickness) of the iron nitride layer

pressure. This is due to the fact that under reduced pressure for the same value of ammonia dissociation degree, the nitrogen flux to the surface is lower than at normal pressure. The volume of nitrogen flux is determined by the disposability of nitrogen in the nitriding atmosphere under the given process conditions (15). The dissociation reaction produces 0.5 mole of nitrogen and 1.5 mole of hydrogen from one mole of ammonia. Knowing the volume of dissociating ammonia, the mass of one mole of nitrogen (28.016 g) and its volume (22.414 dm³), it is possible to calculate the mass of nitrogen obtained from the dissociation reaction:

$$m_{N_2} = P \cdot \frac{\frac{1}{2}V_{NH_3}^*}{22.414} \cdot 28.016 \approx P \cdot 0.625 \cdot V_{NH_3}^* \quad (2)$$

where: $V_{NH_3}^*$ is volume of ammonia dissociating during the nitriding process, P is pressure.

The volume of the inlet atmosphere can be written as:

$$V_W = V_{NH_3}^* + V_{NH_3}^{**} \quad (3)$$

where: V_W is volume of inlet atmosphere, $V_{NH_3}^{**}$ is volume of ammonia that does not dissociate.

Given:

$$V_{NH_3}^* = s \cdot V_W \quad (4)$$

where: s is ratio of ammonia volume in the inlet atmosphere that dissociates, the mass of separated nitrogen obtained from the dissociation reaction can be calculated from the formula:

$$m_{N_2} = P \cdot 0.625 \cdot s \cdot V_W \quad (5)$$

By substituting the volume V_W for its flow rate F_W [dm³/min], the mass of nitrogen obtained over a time unit can be calculated in g/min:

$$m_{N_2}(t) = P \cdot 0.625 \cdot s \cdot F_W \quad (6)$$

The ammonia share by volume in the inlet atmosphere that dissociates is correlated to the dissociation degree as follows:

$$s = \frac{\alpha}{2-\alpha} \quad (7)$$

where: α is degree of ammonia dissociation.

By substituting the Equation 7 into Equation 6, you get the formula for calculating the disposability of nitrogen m_{N_2} as a function of the atmospheric flow rate, the ammonia dissociation degree and the total pressure in the furnace chamber.

$$m_{N_2}(t) = P \cdot 0.625 \cdot \frac{\alpha}{2-\alpha} \cdot F_W \quad (8)$$

Equation 8 shows that at a constant flow rate, which guarantees a constant value of the ammonia dissociation degree, the nitrogen disposability depends on the total pressure in the furnace chamber. This means that at a pressure of 26 hPa, the disposability of nitrogen in the nitriding atmosphere will be almost 40 times lower than in the nitriding process at 1013.25 hPa.

The disposability of nitrogen, apart from the nitrogen potential, is the second important parameter of the nitriding atmosphere, determining primarily the kinetics of the nitrided layer's growth. Nitrogen disposability is of particular importance in processes using NH₃/N₂ inlet atmospheres and in vacuum nitriding processes. In these processes, only the nitrogen disposability unambiguously determines the nitrogen flux to the nitrided surface (16). In the case of the nitriding of alloy steels, guaranteeing the maximum disposability at the steel saturation stage, i.e. until an iron nitride layer is formed, significantly determines the final result of the process. By the time the iron nitride layer is formed, the possibility/absorptive capacity of the steel is the highest; the longer this stage is at the maximum nitrogen flux, the higher surface hardness is obtained. Obtaining higher surface hardnesses in low-pressure processes requires longer process times, which is also associated with the formation of a thicker iron nitride layer.

CONCLUSIONS

Based on the results presented in the study, the following conclusions were drawn:

1. Low-pressure nitriding is a thermochemical treatment that produces nitrided layers with anti-corrosion properties comparable to those obtained in normal pressure processes.
2. The corrosion protection performance of the nitrided layer depends on the thickness of the superficial iron nitride layer. An iron nitride layer thickness equal or higher than 14 μm, obtained in the low-pressure gas nitriding process, guarantees corrosion resistance in an urban environment for up to 5 months.
3. At the same time, the iron nitride layer was found to increase the friction wear resistance of the nitrided steel. Linear wear of the nitrided layer, at the pressure of 200 MPa occurs within the iron nitride layer and is linear throughout the entire test; whereas, at the pressure of 400 MPa – wear accelerates from the beginning of the test.

REFERENCES

1. Sawicki J, Siedlaczek P, Staszczuk A. Fatigue life predicting for nitrided steel - finite element analysis. *Archives of Metallurgy and Materials*. 2018; 63(2): 917–923. <https://doi.org/10.24425/122423>
2. Kusmic D, van Thanh D. Tribological and Corrosion Properties of Plasma Nitrided and Nitrocarburized 42CrMo4 Steel. *IOP Conf Ser: Mater Sci Eng*. 2017; 179: 012046, <https://doi.org/10.1088/1757-899X/179/1/012046>
3. Michalski J. Using nitrogen availability as a nitriding process parameter. *Industrial Heating*. 2012; 10: 63–68.
4. Standard AMS 2759/10A. Automated gaseous nitriding controlled by nitriding potential. SAE; 1999.
5. Zinchenko V.M, Syropyatov V.Y. New possibilities of gas nitriding as a method for anticorrosion treatment of machine parts. *Metal Science and Heat Treatment*; 40(7): 261–265, <https://doi.org/10.1007/BF02474888>
6. Khatkevich V.M, Nikulin S.A, Rozhnov A.B, Rogachev S.O. Mechanical properties and fracture of ferritic corrosion-resistant steels after high-temperature nitriding. *Metal Science and Heat Treatment*. 2015; 57(3–4): 205–209, <https://doi.org/10.1007/s11041-015-9862-x>
7. Kula P, Wołowiec E, Pietrasik R, Dybowski K, Januszewicz B. Non-steady state approach to the vacuum nitriding for tools. *Vacuum*. 2013; 88: 1–7, <https://doi.org/10.1016/j.vacuum.2012.08.001>
8. Wołowiec-Korecka E, Michalski J, Januszewicz B. The stability of the layer nitrided in the low-pressure nitriding process (LPN). *Coatings* 2023; 13: 257–268, <https://doi.org/10.3390/coatings13020257>
9. Betiuk M, Michalski J, Tacikowski J, Łataś Z. Measuring of the thickness of iron nitrides layers. *Inżynieria Powierzchni* 2014; 2: 60–65.
10. Standard PN-EN ISO 9223:2012. Corrosion of metals and alloys. Corrosiveness of atmospheres. Classification, determination and evaluation. 2012.
11. PN ISO 4628-1. Paints and varnishes - Assessment of coating damage - Determination of the amount and size of damage and the intensity of uniform changes in appearance. 2005.
12. Standard PN-83/H-04302. Friction test in the system: 3 rollers - cone. 1983.
13. Hoffmann R, Mittemeijer EJ. Abkühlen nach dem Nitrieren/Nitrocarburieren. *HTM Journal of Heat Treatment and Materials* 2001; 56(3): 155–155, <https://doi.org/10.1515/htm-2001-560303>
14. Jordan D. Vacuum gas nitriding furnace produces precision nitrided parts. *Heat Treating Progress*. 2009; 9: 45–48.
15. Michalski J, Wołowiec-Korecka E. A study of the parameters of nitriding processes. Part 2. *Met Sci Heat Treat*. 2019; 61(5–6): 351–359.
16. Michalski J, Burdyński K, Wach P, Łataś Z. Nitrogen availability of nitriding atmosphere in controlled gas nitriding processes. *Archives of Metallurgy and Materials*. 2015; 60(2): 747–754, <https://doi.org/10.1515/amm-2015-0201>